

Supplemental Data

CYY-1/Cyclin Y and CDK-5 Differentially Regulate Synapse Elimination and Formation for Rewiring Neural Circuits

Mikyong Park, Shigeki Watanabe, Vivian Y. N. Poon, Chan-Yen Ou, Erik M. Jorgensen, and Kang Shen

Inventory of Supplemental Information

Figure S1. DD Synaptic Remodeling Visualized by GFP::RAB-3, related to Figures 2–5, and 7.

Figure S2. SNB-1/synaptobrevin and SNG-1/synaptogyrin Show the Same Mutant Phenotype as RAB-3 for Synaptic Remodeling in DD neurons, related to Figure 1.

Figure S3. CYY-1 and CDK-5 Are Required for Initiating DD Synaptic Remodeling, related to Figure 1.

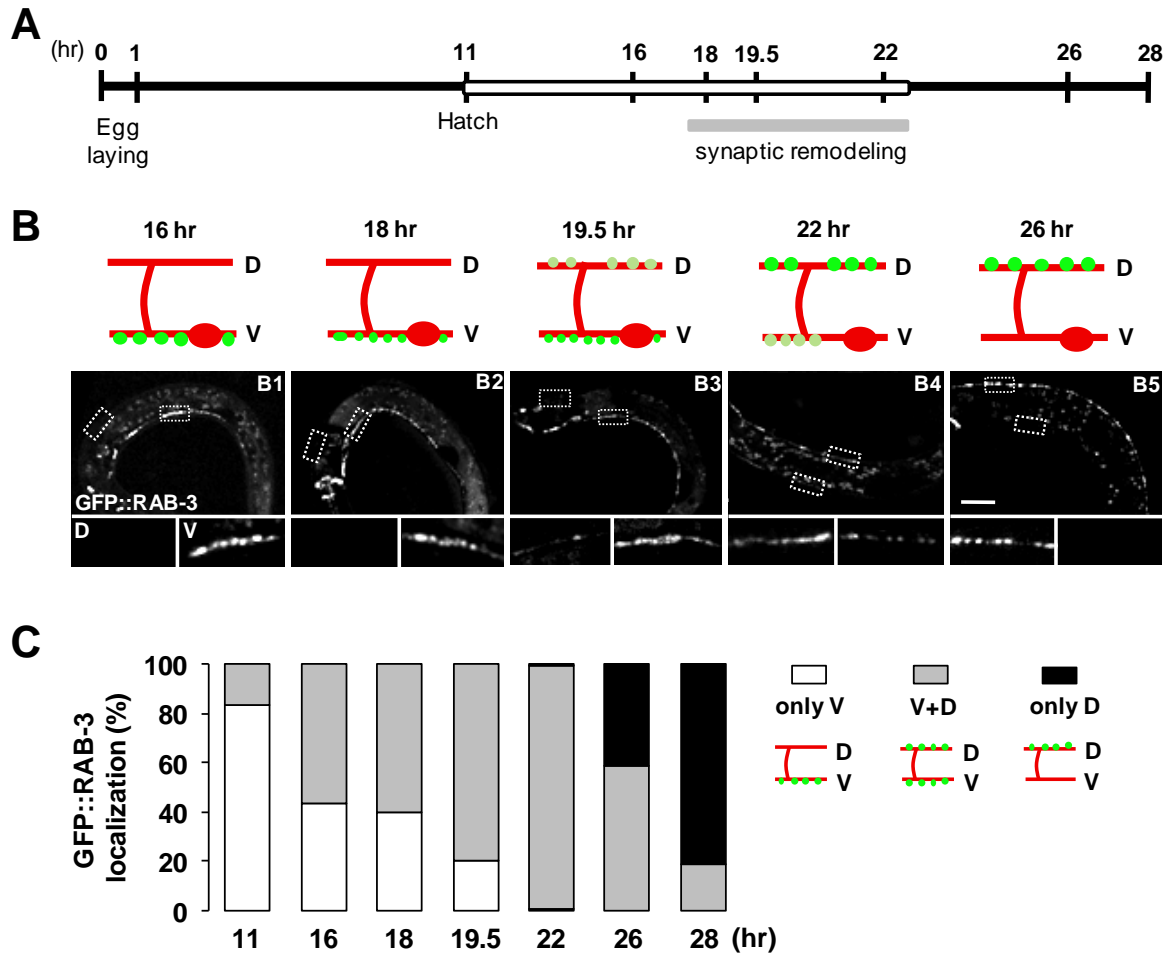
Figure S4. Localization of CYY-1 Shifts to the Ventral Processes Where CYY-1 Acts On During DD Synaptic Remodeling, related to Figure 2.

Figure S5. Ectopic Ventral GFP::RAB-3 Puncta in *cyy-1*, But Not in *cdk-5* Mutants, Exhibit Enhanced Intensity Under the *unc-13* Mutant Background, related to Figure 6.

Figure S6. CDK-5 and UNC-104 Act Together in the New Formation of Dorsal Synapses During DD Remodeling, related to Figure 7.

Figure S7. Model for the Differential Roles of CYY-1 and CDK-5 in DD Synaptic Remodeling

Supplemental Figures and Legends

**Figure S1. DD Synaptic Remodeling Visualized by GFP::RAB-3**

(A) Schematic of experimental timeline. Experiments were performed at 25 °C. See experimental procedures for details. White box denotes the L1 stage.

(B) Progression of synaptic remodeling visualized with GFP::RAB-3 (*wyIs202*). Note the gradual disappearance and appearance of GFP::RAB-3 signals on the ventral and dorsal processes, respectively. Magnified images are shown for representative regions (white dotted boxes) of dorsal (D) and ventral (V) processes. Images were taken at the time points of 16 (B1), 18 (B2), 19.5 (B3), 22 (B4), and 26 (B5) hrs after egg-laying. Schematic diagrams represent the phenotype of GFP::RAB-3 localization in DDs. Green dots represent GFP::RAB-3; light green dots represent weak GFP::RAB-3; red lines denote DD processes and commissures; red ovals,

DD cell bodies; D, dorsal processes; V, ventral processes. All images are oriented anterior to the left and dorsal up unless otherwise mentioned. Scale bar, 20 μm .

(C) Quantification of DD synaptic remodeling based on the GFP::*RAB-3* localization. The X axis indicates the time points since egg-laying. White, gray, and black indicate worms showing GFP::*RAB-3* signals only in the ventral (only V), both in the ventral and dorsal (V+D), and only in the dorsal (only D) sides, respectively, regardless of their intensity. n=139, 170, 177, 207, 217, 144, 104 (from left to right).

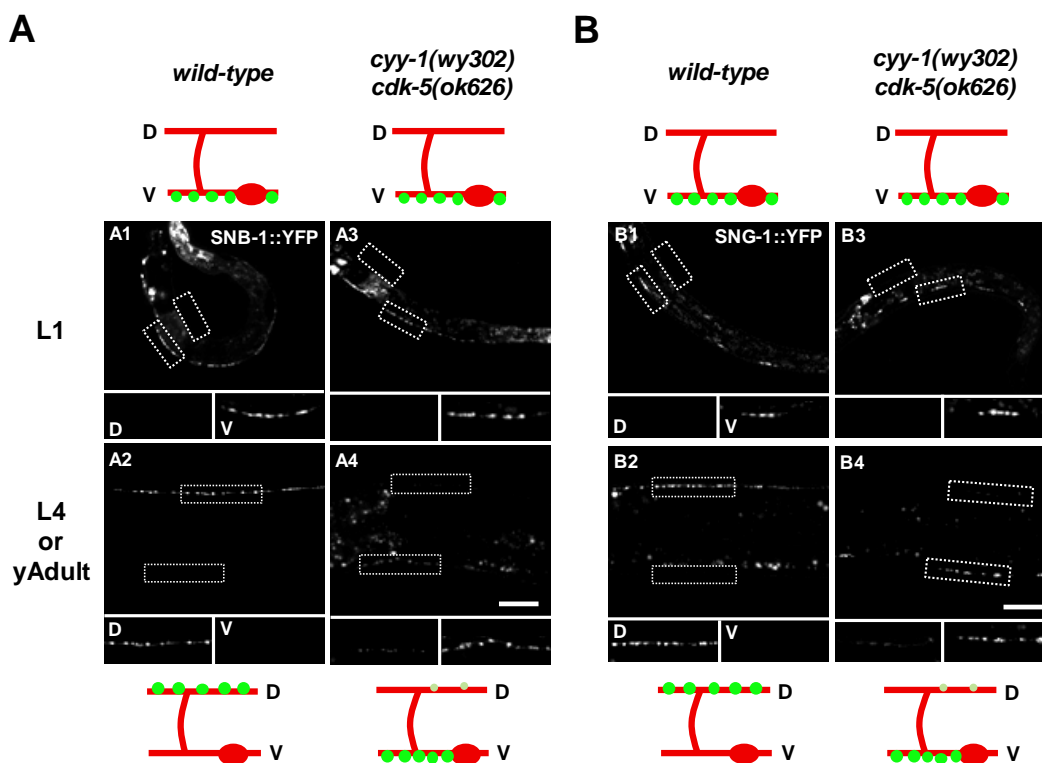


Figure S2. SNB-1/synaptobrevin and SNG-1/synaptogyrin Show the Same Mutant Phenotype as RAB-3 for Synaptic Remodeling in DD neurons

DD synapses are labeled by synaptic vesicle proteins SNB-1/synaptobrevin (A) and SNG-1/synaptogyrin (B). *Wild-type* animals expressing SNB-1::YFP and SNG-1::YFP in DD neurons at the stages of L1 (A1 and B1) and L4 or young adult (A2 and B2). In *cyy-1 cdk-5* double-mutant, most of SNB-1::YFP and SNG-1::YFP puncta are in the ventral processes at the L4 or young adult (A4 and B4). Note that the double-mutants exhibit wild-type localization of SNB-1::YFP and SNG-1::YFP on the ventral side at the stage of L1 (A3 and B3). Schematic diagrams showing phenotypes are shown above and below each image. Green dots, SNB-1::YFP or SNG-1::YFP; red lines, DD ventral and dorsal processes and commissures; red ovals, DD cell bodies; D, dorsal processes; V, ventral processes. Magnified images are shown for representative regions (white dotted boxes) of dorsal (D) and ventral (V) processes. Scale bars, 20 μ m.

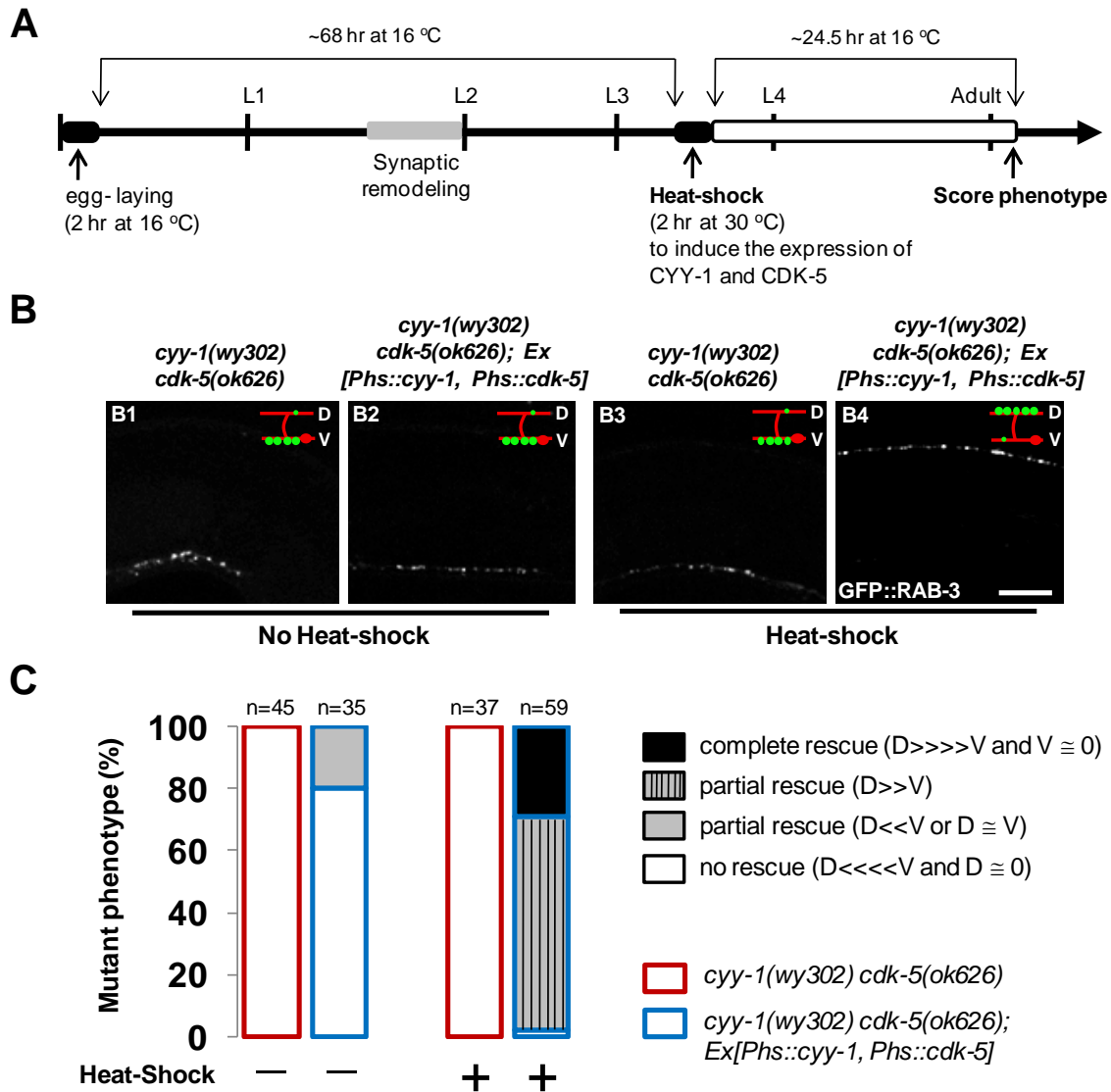


Figure S3. CYY-1 and CDK-5 Are Required for Initiating DD Synaptic Remodeling

(A) Schematic of experimental timeline. See experimental procedures for details.

(B) Induction of both CYY-1 and CDK-5 expression in *cyy-1 cdk-5* double-mutants allows initiation of DD synaptic remodeling. Without heat-shock treatment, in *cyy-1 cdk-5; Ex[Phs::cyy-1, Phs::cdk-5]* worms, DD synaptic remodeling is almost completely blocked (B2) at young adults similar to *cyy-1 cdk-5* double-mutants (B1). Heat-shock induction (2 hours at 30 °C) of CYY-1 and CDK-5 releases the blockade of DD synaptic remodeling (B4). Schematic diagrams showing phenotypes are in the top right in each image. Green dots, GFP-RAB-3; red

lines, DD ventral and dorsal processes and commissures; red ovals, DD cell bodies; D, dorsal processes; V, ventral processes. Scale bar, 20 μm .

(C) Quantification from (B). The degree of rescue, such as complete, partial, or no rescue, is determined based on the intensity of GFP::RAB-3 on ventral (V) and dorsal (D) processes. “No rescue ($D \lllll V$ and $V \cong 0$)” indicates that GFP::RAB-3 intensities of dorsal and ventral processes are similar to those of *cyy-1 cdk-5* double-mutants. “Partial rescue ($D \ll V$ or $D \cong V$)” indicates that dorsal processes have a significant amount of GFP::RAB-3, unlike *cyy-1 cdk-5* double-mutants.

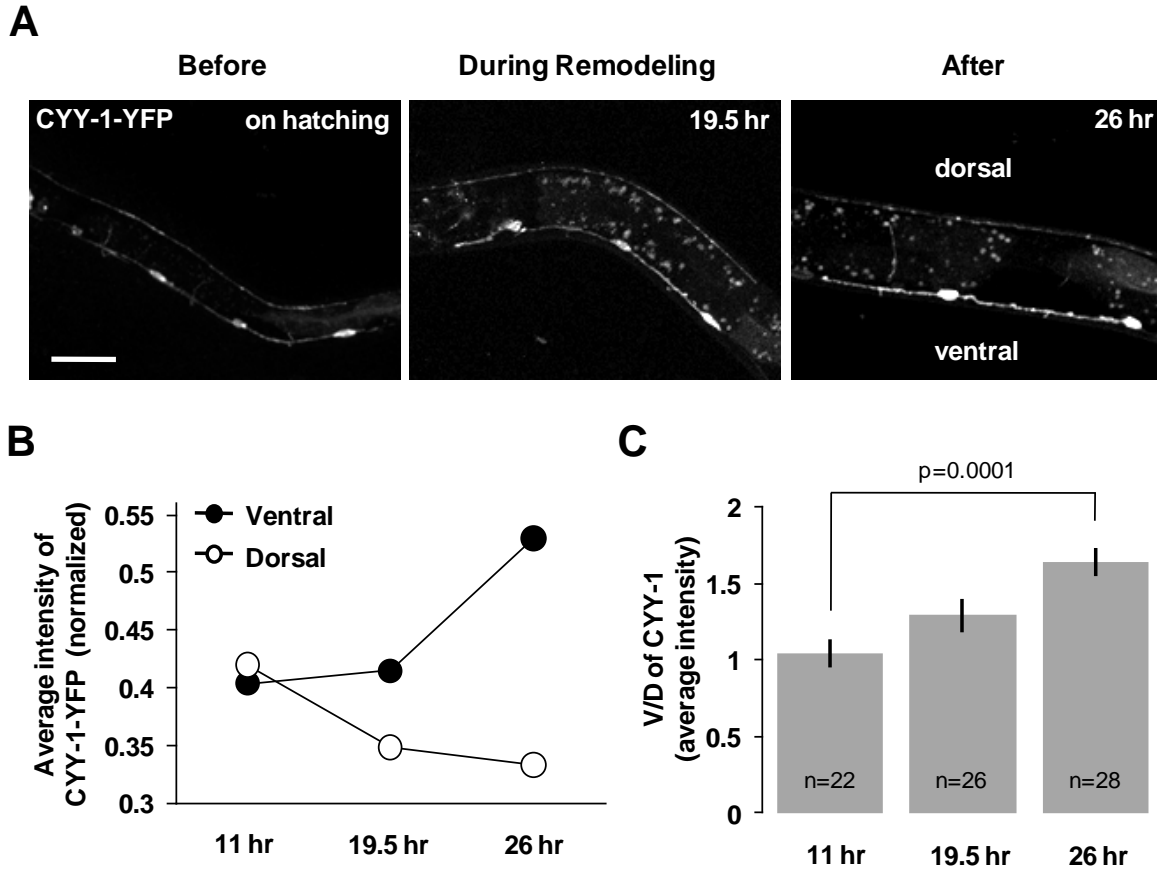


Figure S4. Localization of CYY-1 Shifts to the Ventral Processes Where CYY-1 Acts On During DD Synaptic Remodeling

(A) Distribution pattern of CYY-1-YFP before (left), during (middle), and after (right) synaptic remodeling of DDs. Scale bar, 20 μ m.

(B and C) Quantitative analysis for average intensity of CYY-1-YFP (B) and for the ratio of ventral to dorsal CYY-1-YFP average intensity (C). Error bars, standard error of the mean; Student *t*-test.

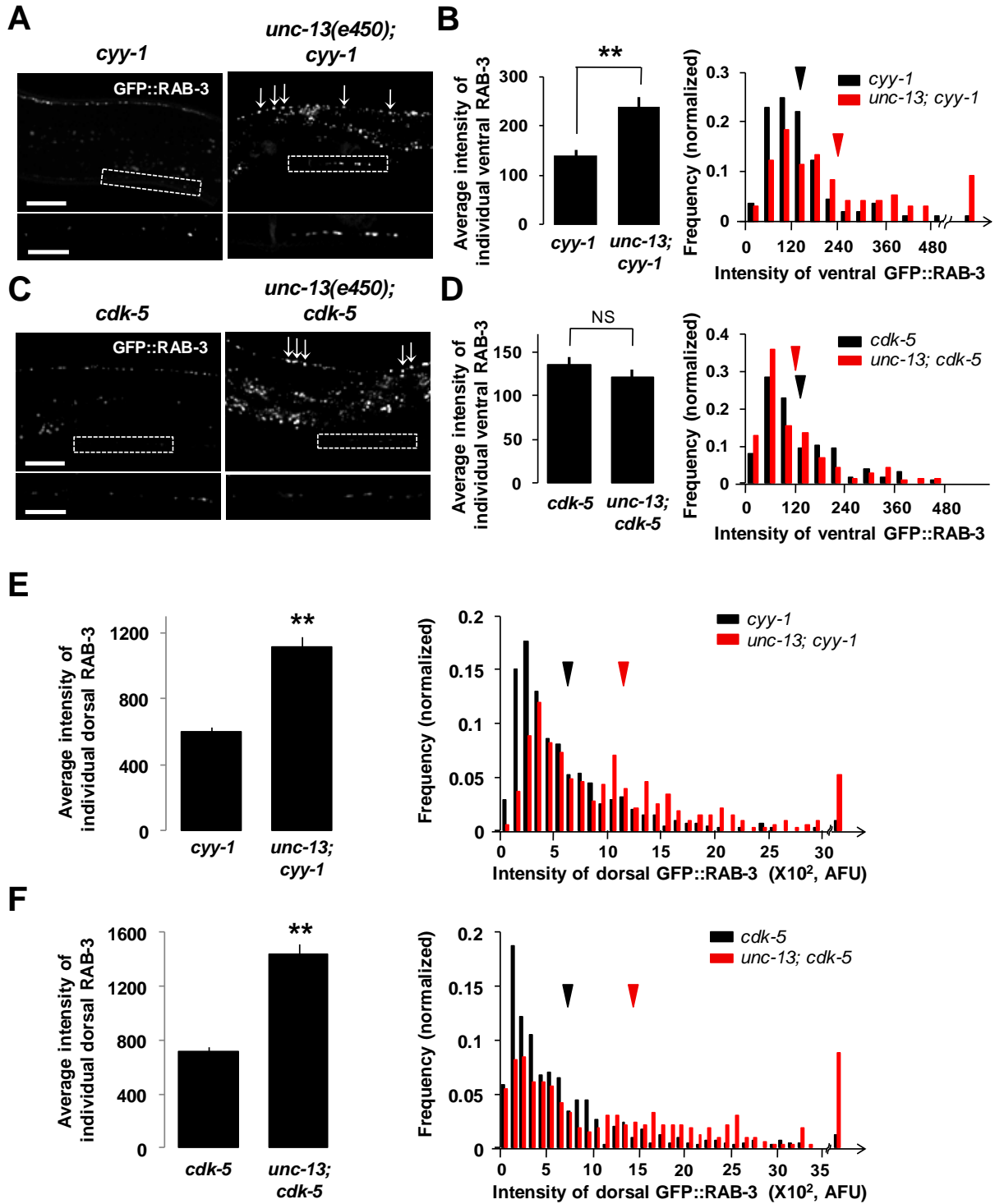


Figure S5. Ectopic Ventral GFP::RAB-3 Puncta in *cyy-1*, But Not in *cdk-5* Mutants, Exhibit Enhanced Intensity Under the *unc-13* Mutant Background

(A) Ventral GFP::*RAB-3* fluorescent intensity in *cyy-1* mutants is enhanced in the *unc-13(e450)* mutant background. Regions containing ventral GFP::*RAB-3* puncta are magnified (white dotted boxes). Imaged and analyzed at the stage of L4.

(B) Quantification of average intensity (left) and histogram analysis (right) of individual ventral GFP::*RAB-3* puncta from Figure 6C. Data represent means \pm SEM. $n=113$ and 97 ventral GFP::*RAB-3* puncta from 20 and 19 worms for *cyy-1* and *unc-13; cyy-1*, respectively. $**p<0.0001$; *Student t-test*. Arrowheads indicate mean values.

(C) Ventral GFP::*RAB-3* fluorescent intensity in *cdk-5* mutants is not enhanced in the *unc-13* mutant background. Regions containing ventral GFP::*RAB-3* puncta are magnified (white dotted boxes). Imaged and analyzed at the stage of L4.

(D) Quantification of average intensity (left) and histogram analysis (right) of individual ventral GFP::*RAB-3* puncta from Figure 6E. Data represent means \pm SEM. $n=126$ and 148 ventral GFP::*RAB-3* puncta from 11 and 11 worms for *cdk-5* and *unc-13; cdk-5*, respectively. NS, not significant; *Student t-test*. Scale bars, 20 and $10 \mu\text{m}$ for low and high magnification images, respectively.

(E and F) Control experiments showing that the intensity of dorsal GFP::*RAB-3* puncta (arrows) in *cyy-1* and *cdk-5* mutants is enhanced under the *unc-13* mutant background. (E) Quantification of average intensity (left) and histogram analysis (right) of individual dorsal GFP::*RAB-3* puncta from Figure S5A. Data represent means \pm SEM. $n=407$ and 328 dorsal GFP::*RAB-3* puncta from 11 and 11 worms for *cyy-1* and *unc-13; cyy-1*, respectively. (F) Quantification of average intensity (left) and histogram analysis (right) of individual dorsal GFP::*RAB-3* puncta from Figure S5C. Data represent means \pm SEM. $n=412$ and 331 dorsal GFP::*RAB-3* puncta from 11 and 11 worms for *cdk-5* and *unc-13; cdk-5*, respectively. $**p<0.0001$, *Student t-test*. Arrowheads indicate mean values. AFU, arbitrary fluorescence units.

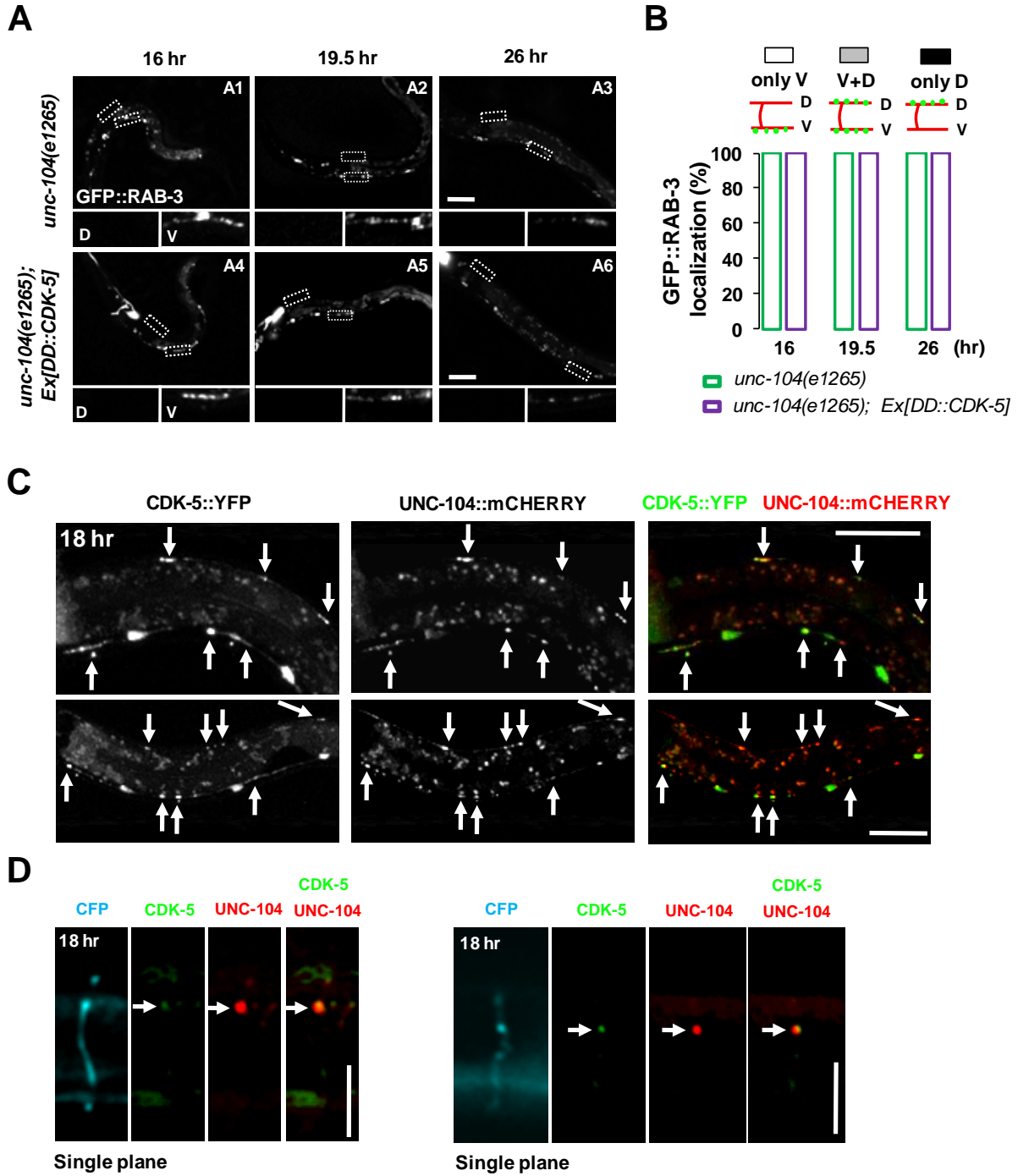


Figure S6. CDK-5 and UNC-104 Act Together in the Formation of New Dorsal Synapses During DD Remodeling

(A and B) UNC-104 is the motor protein responsible for new synapse formation during DD synaptic remodeling. Dorsal synapse formation is completely blocked in the absence of the

motor UNC-104 (D inserts of A1 to A6). D, dorsal processes; V, ventral processes. Scale bars, 20 μm .

(B) Quantification as described in the Figure 3D legend. n (from left to right)=61, 59 (for 16-hr); 52, 44 (for 19.5-hr); 57, 70 (for 26-hr).

(C and D) CDK-5 and UNC-104 colocalize in ventral and dorsal processes and in commissures during DD synaptic remodeling. Two representative images showing colocalization (arrows) of CDK-5-YFP and UNC-104-mCHERRY in the ventral and dorsal processes (C) and commissures (D, single plane) at 18-hr after egg-laying. Cytoplasmic CFP was expressed as a cell-filled cytoplasmic marker. Scale bars, 20 μm .

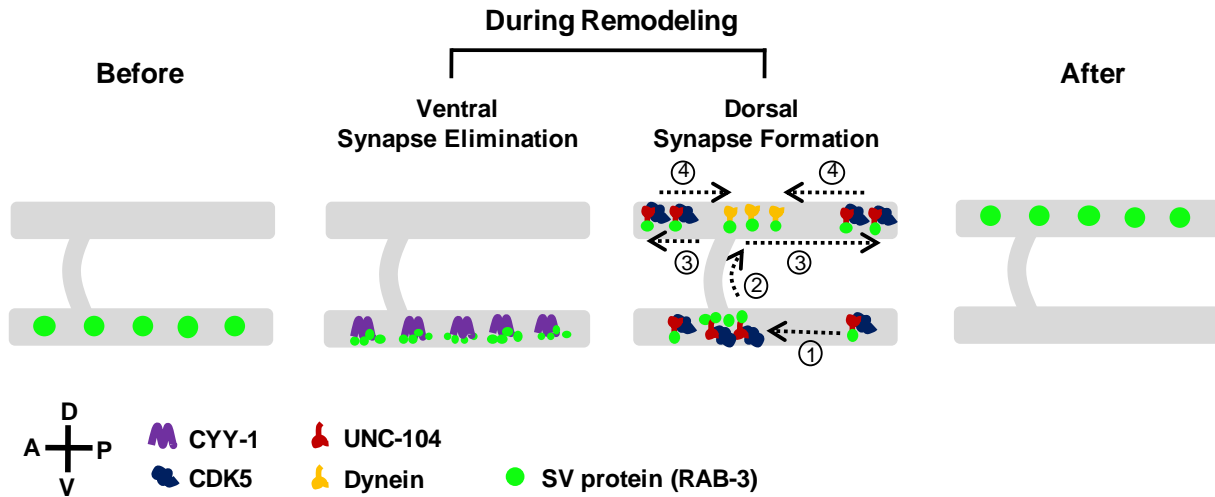


Figure S7. Model for the Differential Roles of CYY-1 and CDK-5 in DD Synaptic Remodeling

CYY-1 mediates ventral synapse disassembly. Then, CDK-5 and UNC-104 are involved in transporting the disassembled ventral synaptic components (①) to the dorsal process via the commissure (②). UNC-104 motor delivers the synaptic components to the anterior and posterior ends of the dorsal process (③). Then, Dynein motor localizes the synaptic components to the proper synaptic sites by delivering them toward anti-ends direction (④). See text for details. A, anterior; P, posterior; D, dorsal; V, ventral.

Experimental Procedures

Strains and Genetics

Worms were maintained on OP50 *E. coli*-seeded nematode growth medium (NGM) plates at 22°C unless otherwise indicated. All strains were generated from N2 Bristol wild-type reference. RB814 *cdk-5(ok626)III*, CB1265 *unc-104(e1265)II*, CB450 *unc-13(e450)I*, and CB3475 *lin-6(e1466)I* strains were obtained through the *Caenorhabditis* Genetics Center.

Molecular Biology

Standard molecular biology techniques were used (details available upon request). Briefly, the *flp-13* promoter fragment (2.28 kb) was obtained by amplifying from genomic DNA. Expression clones were made in a derivative of pPD49.26 (A. Fire), the pSM vector (S. McCarroll and C. I. Bargmann, personal communication). The following plasmids and transgenic strains were generated using standard techniques (Mello and Fire, 1995): *wyIs202(Pflp-13::gfp::rab-3, Pflp-13::mcherry*; an integrant of *wyEx2569*), *wyEx2569(Pflp-13::gfp::rab-3, Pflp-13::mcherry*; 3 and 20 ng μl^{-1} injected, respectively), *wyEx2844(Pflp-13::cyy-1*; 25 ng μl^{-1} injected), *wyEx2889(Pflp-13::cyy-1*; 5 ng μl^{-1} injected), *wyEx2908(Pflp-13::cyy-1::yfp, Pflp-13::mcherry*; 3 and 20 ng μl^{-1} injected, respectively), *wyEx2849(Pflp-13::cdk-5*; 25 ng μl^{-1} injected), *wyEx2866(Pflp-13::cdk-5*; 5 ng μl^{-1} injected), *wyEx2907(Pflp-13::cdk-5::yfp, Pflp-13::mcherry*; 3 and 20 ng μl^{-1} injected, respectively), *wyEx3009(Pflp-13::unc-104*, 25 ng μl^{-1} injected), *wyEx3116(Pflp-13::cdk-5::yfp, Pflp-13::unc-104::mcherry, Pflp-13::cfp*; 10, 10, and 30 ng μl^{-1} injected, respectively), *wyEx2630 (Phs::cyy-1, Phs::cdk-5*; 85 and 53 ng μl^{-1} injected, respectively), *wyEx3147(Pflp-13::dendra2::rab-3*; 50 ng μl^{-1} injected), *wyEx2757(Pflp-13::snb-1::yfp*; 2.5 ng μl^{-1} injected), *wyEx3548(Pflp-13::sng-1::yfp, Pflp-13::cfp*; 2.5 and 25 ng μl^{-1} injected, respectively) and *wyEx3650(Pflp-13::gfp::rab-3, Pflp-13::mcherry::syd-2*; 1.5 and 1.5 ng μl^{-1} injected, respectively). We used the co-injection markers *Podr-1::gfp* or *dsred* injected at 20 ng μl^{-1} or *Pttx-3::mcherry* injected at 50 ng μl^{-1} .

Heat-Shock Experiment

Gravid adult worms of *cyy-1 cdk-5; wyEx2630* were collected and allowed to lay eggs for 2 hours at 16 °C. Eggs were placed at 16 °C for 68 hours to develop (until mid-L3 stage). After

heat-shock for 2 hours at 30 °C to induce CYY-1 and CDK-5, worms were kept for 24.5 hours at 16 °C (until early young adult stage) before the remodeling phenotypes were scored. If GFP::*RAB-3* intensities of dorsal and ventral processes were similar to those of *cyy-1 cdk-5* double-mutants, the animal was categorized as “no rescue ($D \lll V$ and $V \cong 0$)”. If dorsal processes had a significant amount of GFP::*RAB-3*, unlike *cyy-1 cdk-5* double-mutants, the animal was categorized as “partial rescue ($D \ll V$ or $D \cong V$)”.

Confocal Imaging

Confocal images were acquired using a Zeiss LSM510 confocal microscope and a 63x Plan Achromat objective (NA 1.4). Levamisole (5 mM, Sigma) was used to immobilize worms.

Image Analysis and Quantification

Intensity analysis To measure the average fluorescence intensity, the ventral and dorsal processes of DD neurons without the cell bodies were carefully traced and the background intensity subtracted from the intensity in the traced regions using ImageJ. The resultant average intensity of GFP::*RAB-3* from ventral and dorsal processes was normalized to that of cytoplasmic cell-filled mCHERRY from corresponding ventral and dorsal processes for Figures 2E–2G, 3E–3G, 4C–4E, 5C–5E and 7B. The ratio of dorsal to ventral plus dorsal [$D/(V+D)$] GFP::*RAB-3* in Figures 2E, 3E, 4C and 5C was calculated by the following formula: average intensity of dorsal GFP::*RAB-3* / (average intensity of ventral GFP::*RAB-3* + average intensity of dorsal GFP::*RAB-3*). The n values correspond to the number of individual worms.

For the analysis of photoconverted experiments (Figure 5G), the integrated intensity of photoconverted red fluorescence of *RAB-3* in the ventral (V) and the dorsal (D) process at 8-10 hr after UV irradiation was normalized to the integrated intensity of photoconverted red fluorescence of *RAB-3* in the ventral process right after UV irradiation in *wild-type*, *cyy-1*, or *cdk-5* mutant worms.

For ventral GFP::*RAB-3* puncta intensity analysis in *cyy-1, unc-13*; *cyy-1, cdk-5, unc-13*; *cdk-5* mutants (Figures S5A–S5D), L4 worms containing ventral GFP::*RAB-3* puncta were imaged. Images were thresholded and the integrated intensity of individual GFP::*RAB-3* puncta was measured using ImageJ. Same methods were applied for dorsal GFP::*RAB-3* puncta analysis in *cyy-1, unc-13*; *cyy-1, cdk-5, unc-13*; *cdk-5* mutants (Figures S5E and S5F).

For colocalization analysis of ventral GFP::RAB-3 and mCHERRY::SYD-2 in *cyy-1* and *cdk-5* mutants (Figure 6B), L4 worms containing ventral GFP::RAB-3 puncta were imaged and the percentage of ventral GFP::RAB-3 puncta overlapping mCHERRY::SYD-2 was quantified. For colocalization analysis of ventral SNB-1::CFP and UNC-49::YFP in *cyy-1* and *cdk-5* mutants (Figure 6D), L3–young adult worms containing ventral SNB-1::CFP puncta were imaged and the percentage of ventral SNB-1::CFP puncta overlapping UNC-49::YFP was quantified.

Electron Microscopy

Dorsal nerve cord D type neuron (DD) is reconstructed and analyzed from N2 *wild-type* and *cyy-1 cdk-5* animals as previously described (Ou et al., 2010). Prior to high pressure freezing, a type-A specimen carrier was filled with bacteria (OP50), and nematodes were placed on the top the bacteria. A type-B specimen carrier, which was dipped in hexadecane, was used as a cap to ensure no air bubbles in the cup. The specimens are rapidly frozen in a high pressure freezer (HPM010, BAL-TEC) and submerged into a liquid nitrogen bath. Under the liquid nitrogen, the specimen was transferred into fixatives (1% osmium tetroxide 0.1% uranyl acetate in anhydrous acetone), which was pre-mixed and pre-frozen in cryogenic vials. The vitreous ice in the tissues are substituted with acetone while the tissues were fixed and stained in an automated freeze-substitution unit (AFS2, Leica microsystem). The program was set as follows: 48 hours at -90°C, 5°C/hour to -20°C (14 hours), 16 hours at -20°C, and 10°C/hour to 20°C (4 hours). Following the freeze-substitution, specimens were infiltrated with and subsequently embedded in plastic, epon-araldite. The anterior reflex of gonad was located, and 200-300 serial sections were cut using a microtome (Ultracut 6, Leica microsystem) and photographed using a transmission electron microscopy (H-7100, Hitachi) and a digital camera (orius, GATAN). The DD neurons were identified by their position and orientation within the dorsal nerve cord. A varicosity was defined as a series of profiles with an area larger than 10,000 square nm regardless of the existence of dense projections.

Reference

Mello, C., and Fire, A. (1995). DNA transformation. *Methods Cell Biol* 48, 451-482.

Figure Legends**Figure 2. CYY-1 Is Required for the Completion of DD Synaptic Remodeling**

(D) n (from left to right)= 121, 130, 127, 41 (for 16-hr); 119, 125, 138, 56 (for 18-hr); 107, 157, 133, 67 (for 19.5-hr); 124, 127, 138, 45 (for 22-hr); 137, 122, 132, 48 (for 26-hr).

(E, F, and G) n (from left to right)= 9, 6, 9 (for 16-hr); 17, 20, 20 (for 19.5-hr); 11, 10, 15 (for 22-hr); 11, 11, 20 (for 26-hr).

Figure 3. CDK-5 Is Required for the Completion of DD Synaptic Remodeling

(D) n (from left to right)= 240, 102, 82, 67 (for 16-hr); 254, 70, 179, 50 (for 18-hr); 324, 108, 187, 85 (for 19.5-hr); 346, 99, 87, 64 (for 22-hr); 222, 106, 101, 59 (for 26-hr).

(E, F, and G) n (from left to right)= 18, 19, 10 (for 16-hr); 27, 24, 10 (for 19.5-hr); 14, 6, 11 (for 22-hr); 11, 11, 17 (for 26-hr).

Figure 4. CYY-1 and CDK-5 Play Differential Roles During DD Synaptic Remodeling

(B) n (from left to right)= 170, 90, 82, 132 (for 16-hr); 177, 123, 179, 215 (for 18-hr); 207, 108, 187, 174 (for 19.5-hr); 217, 103, 87, 85 (for 22-hr); 144, 47, 101, 41 (for 26-hr).

(C, D, and E) n (from left to right)= 18, 6, 8, 14 (for 16-hr); 18, 20, 10, 10 (for 19.5-hr); 14, 10, 10, 18 (for 22-hr); 11, 11, 11, 19 (for 26-hr).

Figure 5. CYY-1 Contributes to the Function of CDK-5 to Form Dorsal Synapses During DD Synaptic Remodeling

(B) n (from left to right)= 240, 102, 104, 103 (for 16-hr); 254, 70, 127, 85 (for 18-hr); 324, 108, 149, 121 (for 19.5-hr); 346, 99, 198, 87 (for 22-hr); 222, 106, 110, 63 (for 26-hr).

(C, D, and E) n (from left to right)= 9, 19, 13, 23 (for 16-hr); 17, 24, 15, 14 (for 19.5-hr); 11, 6, 11, 11 (for 22-hr); 6, 11, 20, 21 (for 26-hr).

Figure 7. CDK-5 and UNC-104/Kinesin3 Act Together To Form New Dorsal Synapses During DD Remodeling

(C) n (from left to right)=240, 67, 82, 97 (for 16-hr); 254, 73, 179, 80 (for 18-hr); 324, 60, 187, 81 (for 19.5-hr); 346, 70, 87, 71 (for 22-hr); 222, 114, 101, 120 (for 26-hr).